APPLIED AND ENVIRONMENTAL MICROBIOLOGY, Sept. 2000, p. 3705–3710 Vol. 66, No. 9
0099-2240/00/$04.00+0

Role of *phaD* in Accumulation of Medium-Chain-Length Poly(3-Hydroxyalkanoates) in *Pseudomonas oleovorans*

STEFAN KLINKE, GUY DE ROO, BERNARD WITHOLT,* AND BIRGIT KESSLER

Institute of Biotechnology, Swiss Federal Institute of Technology, CH-8093 Zurich, Switzerland

Received 2 December 1999/Accepted 16 June 2000

Pseudomonas oleovorans **is capable of producing poly(3-hydroxyalkanoates) (PHAs) as intracellular storage material. To analyze the possible involvement of *phaD* in medium-chain-length (MCL) PHA biosynthesis, we generated a *phaD* knockout mutant by homologous recombination. Upon disruption of the *phaD* gene, MCL PHA polymer accumulation was decreased. The PHA granule size was reduced, and the number of granules inside the cell was increased. Furthermore, mutant cells appeared to be smaller than wild-type cells. Investigation of MCL PHA granules revealed that the pattern of granule-associated proteins was changed and that the predominant protein PhaI was missing in the mutant. Complementation of the mutant with a *phaD*-harboring plasmid partially restored the wild-type characteristics of MCL PHA production and fully restored the granule and cell sizes. Furthermore, PhaI was attached to the granules of the complemented mutant. These results indicate that the *phaD* gene encodes a protein which plays an important role in MCL PHA biosynthesis. However, although its main effect seems to be the stabilization of MCL PHA granules, we found that the PhaD protein is not a major granule-associated protein and therefore might act by an unknown mechanism involving the PhaI protein.**

Polyhydroxyalkanoates are storage polymers accumulated by a wide variety of bacteria under conditions of nutrient limitation and carbon excess (25). *Pseudomonas oleovorans* produces medium-chain-length (MCL) poly(3-hydroxyalkanoates) (PHAs), which are composed of monomers with a chain length varying from 6 to 14 carbon atoms, when grown on fatty acids (5, 14). PHAs are under investigation because of their potential as biodegradable polymers produced from renewable resources (1, 24).

Three different types of proteins are involved in the synthesis and degradation of PHAs and in the assembly or maintenance of intracellular PHA granules (26): PHA synthases, PHA depolymerases, and phasins. The group of granule-associated proteins named phasins show analogies to oleosins, a class of amphipathic proteins that form a layer at the surfaces of triacylglycerol inclusions found in seeds and pollen of plants (8, 17).

In *P. oleovorans* GPo1 the major MCL PHA biosynthesis genes are clustered in the PHA locus: two synthase-encoding genes are separated by an open reading frame (ORF) that encodes a depolymerase. Downstream of the second synthase-encoding gene is a fourth ORF (*phaD*) (9), for which a role in PHA biosynthesis has not yet been described. Recently, two additional genes downstream of *phaD*, encoding the PhaI and PhaF proteins, have been identified (20). PhaF and PhaI are major PHA granule binding proteins (20). Moreover, PhaF behaves as a negative regulator of *phaC1* gene expression.

Sequence alignments of PhaD with protein databases revealed no significant homology to PHA synthases or PHA depolymerases. Additionally, no homology between PhaD and other phasins, which themselves do not show significant homology within their group, was detected. However, Valentin et al. reported that deletion of *phaD* in addition to inactivation of *phaI* and *phaF*, encoding the major granule-associated proteins of *Pseudomonas putida*, lead to a significant decrease in MCL PHA accumulation (27).

In this study, we investigated the role of *phaD* in MCL PHA biosynthesis in *P. oleovorans*. A *phaD* knockout mutant was negatively affected in PHA biosynthesis, despite the fact that the PhaD protein was not associated with PHA granules.

TABLE 1. Bacterial strains and plasmids

Strain or plasmid	Description	Reference(s)
P. oleovorans strains		
GPo12	OCT plasmid$^-$, PHA$^+$	11, 23
GPo1000	OCT plasmid$^-$, PHA$^+$ Rf^r	This study
GPo1001	OCT plasmid$^-$, PHA$^+$ Rf^r Tc^r *phaD*Ω(8bp::*tet*)	This study
E. coli strains		
S17-1 λ*pir*	RP4:2-Tc:Km Tn*7* λ*pir* Sm^r Tp^r	16
HB101	F$^-$ Δ(*gpt-proA*)*62 leuB6 supE44 ara-14 galK2 lacY1 xyl-5 recA13*	22
Plasmids		
pGEc404	Km^r Sm^r; RSF1010 *ori*, Mob$^+$ *phaC2 phaD* pJRD215	9
pGEc420	Ap^r Sm^r; f1 *ori*, *lacZ phaC2 phaD*, pGEM-7Zf(+)	9
pUT mini-Tn*5* Tc	Ap^r Tc^r; delivery plasmid for mini-Tn*5* Tc	3, 4
pRK600	Cm^r; ColE1 ori, RK2-Mob$^+$ RK2-Tra$^+$	4
pBCKS	Cm^r; ColE1 ori, *lacZ*, f1 ori, pUC19	M. A. Prieto, personal communication
pVLT33	Km^r; RSF1010-*lacI*^{q}/*tacp*	2
pGEc420-*phaD*::*tet*	Tc^r; *phaD*Ω(8bp::*tet*), pGEc420	This study
pUT-*phaD*::*tet*	Tc^r; *phaD*Ω(8bp::*tet*), pUT	This study
pHAD2	Cm^r; *phaD*, pBCKS	This study
pHAD5	Km^r; *phaD*, pVLT33	This study

* Corresponding author. Mailing address: Institute of Biotechnology, Swiss Federal Institute of Technology, ETH Zurich, Hoenggerberg HPT, CH-8093 Zurich, Switzerland. Phone: 41-1-633 3286. Fax: 41-1-633 1051. E-mail: bw@biotech.biol.ethz.ch.

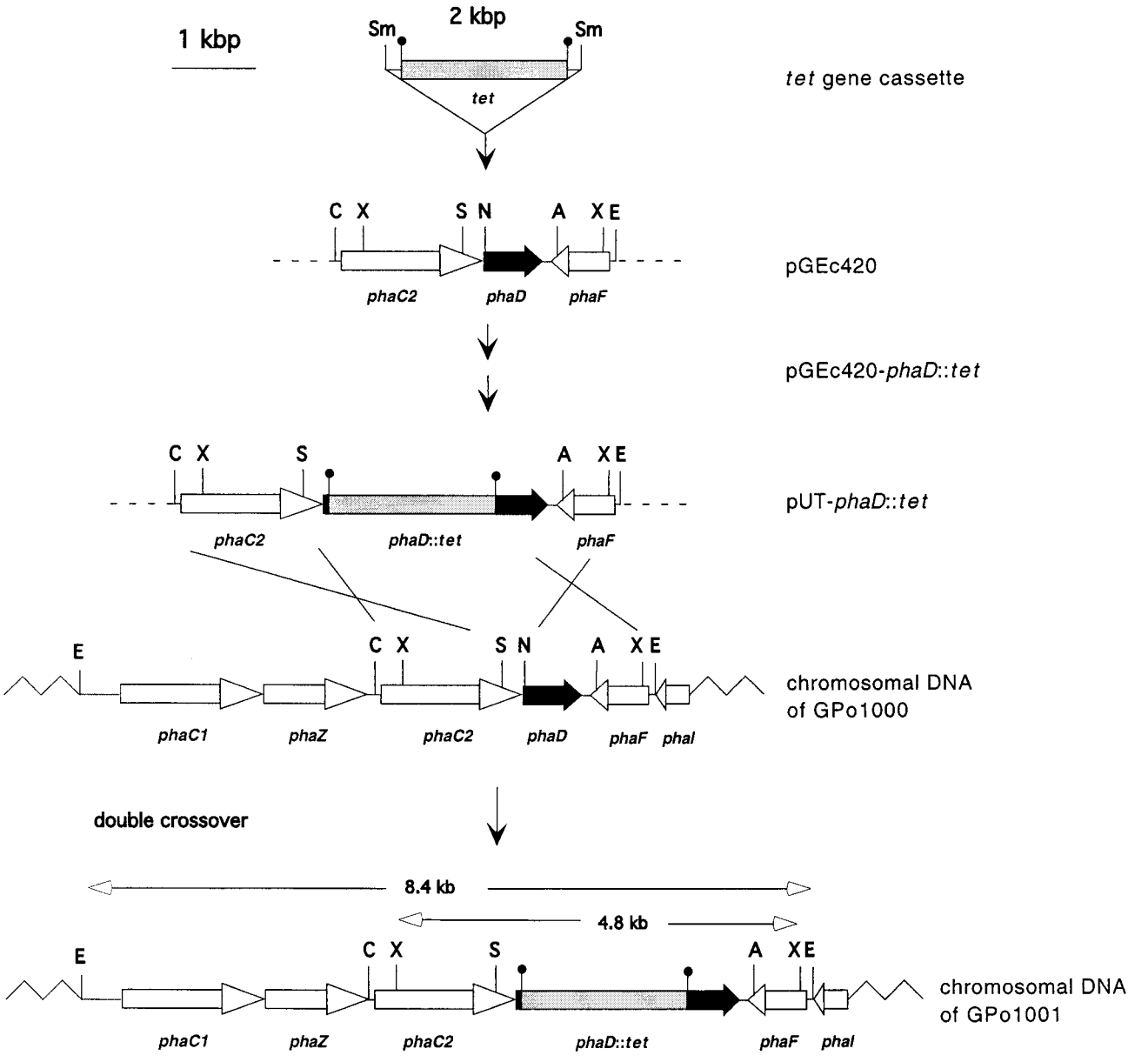

FIG. 1. *phaD* gene replacement by homologous recombination in *P. oleovorans* GPo1000. The upper three lines show the construction of the plasmid pUT-*phaD*::*tet*, which was used for gene replacement of *phaD*. A double crossover between pUT-*phaD*::*tet* and homologous DNA in the chromosome of *P. oleovorans* GPo1000 resulted in the *phaD*::*tet*-integrated strain GPo1001. Gray box, *tet* resistance gene; black bar, *phaD* gene; open arrows, other genes up- and downstream of the *phaD* gene. Abbreviations: A; *Asp*718, C; *Cla*I, E; *Eco*RI, N; *Nru*I, S; *Stu*I, Sm; *Sma*I; X; *Xmn*I.

MATERIALS AND METHODS

Bacterial strains, plasmids, and growth conditions. *Pseudomonas* strains were grown at 30°C in minimal medium E2 (14) with addition of 0.2% (wt/vol) citrate for precultures. To stimulate PHA production, cells were grown in minimal medium 0.1NE2 with addition of 15 mM octanoate. *Escherichia coli* strains were grown at 37°C in complex Luria-Bertani medium (22). Cells were cultivated in Erlenmeyer flasks and incubated at 225 rpm. Antibiotics were added as needed at the following concentrations (micrograms per milliliter): piperacillin, 100; tetracycline, 12.5; rifampin, 30; and kanamycin, 100. Media were solidified with 1.5% (wt/vol) agar for plate experiments. Cell densities were measured spectrophotometrically as optical density at 450 nm (OD_{450}) (30). Cultures were harvested by centrifugation and washed with 10 mM $MgSO_4$. For determination of PHA, the cell pellet was lyophilized. The strains and plasmids used are listed in Table 1.

Construction of a *phaD* insertion mutant. Basic recombinant DNA techniques were carried out essentially as described by Sambrook et al. (22). A rifampin-resistant mutant of GPo12, named GPo1000, was generated by growing *P. oleovorans* GPo12 on rifampin for several cycles. This strain showed a PHA accumulation phenotype identical to that of the parental strain GPo12 (data not shown). GPo1000 was used for insertional inactivation of the *phaD* gene by gene replacement using the tetracycline resistance gene cassette (*tet*).

The *tet* gene (2 kbp) was isolated by digesting plasmid pUT mini-Tn*5* Tc with *Sma*I and cloned into the *Nru*I site of pGEc420, which was made blunt with nuclease S1. The resulting vector, called pGEc420-*phaD*::*tet* (Fig. 1), contains the *tet* gene inserted 8 nucleotides downstream of the start codon of the *phaD* gene. Because of strong terminators up- and downstream of the *tet* gene (4), transcription of the complete *phaD* gene is inhibited in this construct. Plasmid pGEc420-*phaD*::*tet* was digested with *Cla*I, made blunt with nuclease S1, and then digested with *Eco*RI. The *Eco*RI-blunt fragment, consisting of *phaC2*, *phaD* with the *tet* insertion, and *phaF*, was ligated to the pUT backbone, resulting in plasmid pUT-*phaD*::*tet* (Fig. 1). By mating of donor strain *E. coli* S17-λ*pir* pUT-*phaD*::*tet* and recipient strain *P. oleovorans* GPo1000, the plasmid pUT-*phaD*::*tet* was transferred into the recipient strain. Selection was done on Luria-Bertani plates with tetracycline and rifampin to obtain cells in which homologous

recombination had occurred. To select only clones with a double recombination event, cells were screened on the β-lactam antibiotic piperacillin to select for strains which lost their β-lactam antibiotic resistance-transferring pUT plasmid. One mutant of *P. oleovorans* GPo1000, named GPo1001, was found to exhibit the desired phenotype of rifampin and tetracycline resistance and piperacillin sensitivity. This was presumed to be due to replacement of the wild-type *phaD* gene in the chromosome by the *tet* gene-disrupted *phaD* from pUT-*phaD*::*tet*, as a result of homologous recombination involving a double crossover followed by loss of the plasmid (Fig. 1).

Verification of the *P. oleovorans* GPo1001 genotype. Southern blot analysis was performed by using either a 2-kb *tet* gene fragment, obtained by *Sma*I digestion of pUT mini-Tn*5* Tc, or a 0.6-kb *phaD* internal fragment, amplified by PCR using the primers 5′-CCGCGACACCGAATCAACAGGCTTAC-3′ and 5′-ATGAA GACTCGCGACCGTATCCTC-3′. Both probes were labeled using a digoxigenin labeling and detection kit (Boehringer Mannheim). Hybridization of an *Eco*RI or *Xmn*I digest of chromosomal DNA using *phaD* as a probe showed a single 6.4- or 2.8-kb fragment in GPo1000, respectively. In the *phaD*::*tet* mutant a hybridization signal at 8.4 or 4.8 kb was detected, consistent with the size expected from insertion of the 2-kb *tet* resistance cassette into the 6.4- or 2.8-kb fragment containing the native *phaD* gene (data not shown). When the *tet* cassette was used to probe the same digest, a 8.4-kb (*Eco*RI) or 4.8-kb (*Xmn*I) fragment was detected in the *phaD*::*tet* mutant, providing evidence that this fragment contains *phaD*::*tet*. As expected, no hybridization of the *tet* probe was seen with GPo1000 chromosomal DNA (data not shown).

Construction of a broad-host-range *phaD* expression plasmid. Plasmid pGEc404 was digested with *Stu*I and *Asp*718, generating a 1-kb fragment containing *phaD* which was cloned into vector pBCKS digested with *Eco*RV and *Asp*718. The resulting construct, named pHAD2, was sequenced in order to verify the *phaD* gene sequence. Subsequently, pHAD2 was digested with *Eco*RI and *Asp*718. Prior to ligation, the ends of this fragment were dephosphorylated with arctic shrimp alkaline phosphatase, followed by cloning into *Eco*RI- and *Asp*718-digested pVLT33, a broad-host-range vector. This construct, containing the *phaD* ORF downstream of a *tac* promoter, was named pHAD5.

PHA determination. Analysis of PHA accumulation and composition was performed essentially as described before (10).

Electron microscopy and analysis of electron micrographs. Stationary-phase cultures (27 h of growth) were prepared for electron microscopy by high-pressure freezing and freeze substitution as described previously (7). The cells were taken up in cellulose capillaries (type LD OC 02, Microdyn. Wuppertal, Germany) and were subjected to high-pressure freezing (high-pressure freezing machine 010, BAL-TEC AG, FL-9496 Balzers). The frozen samples were stored in liquid nitrogen until further use. Freeze substitution was performed in anhydrous acetone containing 2% osmium tetroxide (28). The samples were plastic embedded in Epon-Araldite, sectioned on a Reichert Jung Ultracut E microtome equipped with a diamond knife (Diatome AG, Biel, Switzerland), stained with uranyl acetate and lead citrate (21), and examined in an H-600 transmission electron microscope (Hitachi, Tokyo, Japan).

To determine the volume of PHA granules from the micrographs, 22 cells of the wild type and 14 cells of the mutant were selected, in which the PHA granule radius was measured. We analyzed 31 granules of the wild type and 46 of the mutant. Only granules with sharp boundaries were selected. Round granules were assumed to be spherical (volume = $4/3\pi r^3$), whereas oval granules were assumed to be ellipsoidal (volume = $4/3\pi a^2 b$). The number of PHA granules per cell was determined only for cells which were fully visible in the electron micrographs. We selected 23 wild-type cells and 52 mutant cells. Cell volumes were determined as described above for PHA granule volume determination, and the ratio of these volumes was calculated using 23 cells of the wild type and 14 cells of the mutant.

The granule volumes, the number of granules per cell, and the ratio of granule volume to cell volume for wild-type and mutant cells were compared. The data were analyzed with the software package S-Plus using the two-sample *t* test and the Wilcoxon rank sum test.

Granule isolation and analysis of granule-associated proteins. PHA granules were isolated on a sucrose gradient as previously reported (12). Samples of purified granules were mixed 1:1 (vol/vol) with sodium dodecyl sulfate-polyacrylamide gel electrophoresis (SDS-PAGE) loading buffer, and the bound proteins were separated on SDS-polyacrylamide gels as described before (13). The proteins were electroblotted directly from a gel onto a polyvinylidene difluoride membrane. The amino-terminal sequences were determined by Edman degradation using a G 1000 A automated protein sequencer (Hewlett-Packard).

RESULTS

Analysis of *P. oleovorans* GPo1001 PHA biosynthesis. To investigate whether the *phaD* mutation affects the PHA biosynthesis pattern, we determined time-dependent PHA accumulation by *P. oleovorans* GPo1001 and its parental strain *P. oleovorans* GPo1000 (Table 2). We found that cell growth and polymer accumulation by GPo1001 were significantly lower than those by the parental strain GPo1000; the polymer accumulated by GPo1001 never amounted to more than 20% of that synthesized by GPo1000. Moreover, the difference in PHA accumulation between the strains increased with time, varying from 55 to 58% (wt/wt) PHA in GPo1000 and from 10 to <2% (wt/wt) in GPo1001 between 23 and 46 h of growth, indicating a nearly complete intracellular depolymerization of the PHA within the observed incubation time in GPo1001. The PHA monomer compositions were similar in the mutant and the wild type during the observed period and showed 3-hydroxyoctanoate as the predominant monomer in both strains (Table 2).

TABLE 2. PHA contents and monomer compositions of *P. oleovorans* GPo1000 and the *phaD* insertion mutant *P. oleovorans* GPo1001 cultivated on octanoate[a]

Organism	Time (h)	Cell dry wt (g liter^{-1})	PHA (%, wt/wt)	PHA monomer composition[b] (mol%)		
				C_6	C_8	C_{10}
GPo1000	23	0.74	54.9	7.7	92.3	<0.1
	27	0.77	56.1	7.7	92.3	<0.1
	46	0.86	58.3	7.5	92.5	<0.1
GPo1001	23	0.44	9.6	6.0	94.0	<0.1
	27	0.42	8.9	6.4	93.6	<0.1
	46	0.35	1.1	8.5	91.5	<0.1
GPo1001/pHAD5[3]	23	0.79	38.9	6.3	93.5	0.2
	27	0.94	43.8	6.5	93.3	0.2
	46	0.94	30.7	3.3	91.3	5.4

[a] Cells were cultivated in 0.1NE2 minimal medium with 15 mM octanoate. After 23, 27, and 46 h of cultivation, cells were harvested and lyophilized, and the PHA composition was measured by GC.
[b] C_6, 3-hydroxyhexanoate; C_8, 3-hydroxyoctanoate; C_{10}, 3-hydroxydecanoate.
[c] Cells were grown until they reached the exponential phase (OD_{450} = 0.2) and then induced with 0.5 mM IPTG.

Analysis of *P. oleovorans* GPo1000 and GPo1001 PHA granule characteristics. Cells and PHA granules of the wild type and the mutant differed significantly in their appearance as observed by transmission electron microscopy (Fig. 2A and B). Table 3 shows that the median PHA granule volume decreased by 3 orders of magnitude in the *P. oleovorans* mutant GPo1001 compared to the wild-type *P. oleovorans* GPo1000. The mutant GPo1001 had a higher number of PHA granules per cell (median = 5) than the wild-type GPo1000 (median = 1). As a result, the ratio of granule volume to cell volume for GPo1001 cells decreased significantly (median = 2%) compared to that for GPo1000 cells (median = 49%). The difference found for the granule volume, the granule numbers, and the ratio of granule volume to cell volume were statistically significant according to the *t* test and the Wilcoxon rank sum test. Moreover, we found a reasonable agreement between the amounts (percentage, weight/weight) of PHA for the mutant and wild type derived from electron micrographs and determined by GC measurements (Table 3).

Influence of *phaD* gene disruption on granule-associated proteins. SDS-PAGE analysis of isolated granules showed that PhaD is not a major granule-associated protein. Interestingly, we found that the patterns of granule-associated proteins of GPo1000 and GPo1001 differed significantly. The most obvious difference was a missing protein band in granule preparations of the *phaD* insertion mutant GPo1001 at 18 kDa (Fig. 3). The N terminus of this 18-kDa protein in GPo1000, XKVT VKKKDDAPGTLGEVRGYARKIMLAGIGAYARVGQ EG, is, except for two amino acids, identical to that of PhaI,

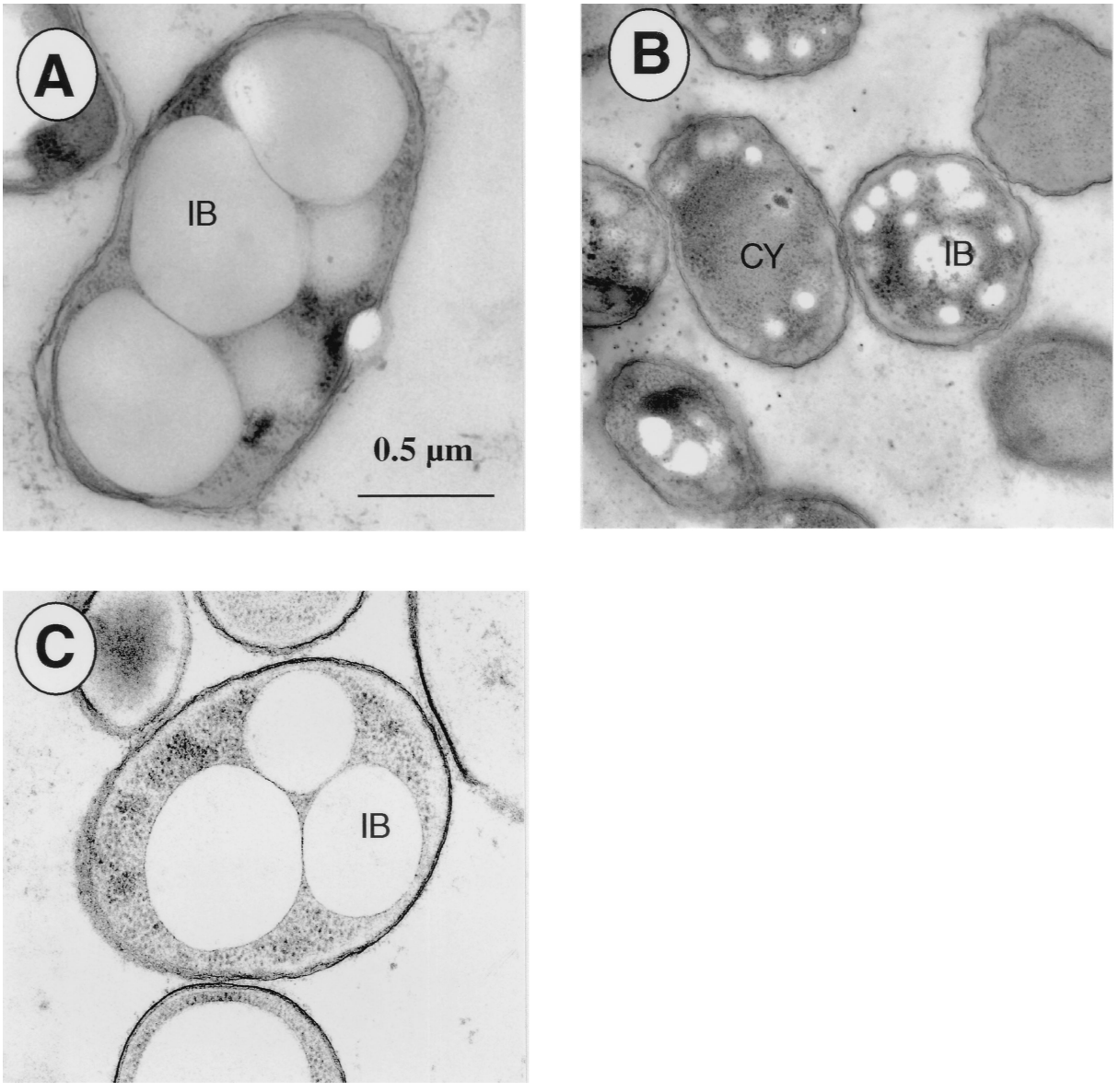

FIG. 2. Morphology of *P. oleovorans* GPo1000 and GPo1001. Cells were cultivated in 0.1NE2 minimal medium containing 15 mM octanoate and were harvested in the stationary growth phase. Electron micrographs were obtained as described in Materials and Methods and depict representative cells. (A) *P. oleovorans* GPo1000. (B) *P. oleovorans* GPo1001. (C) *P. oleovorans* GPo1001(pHAD5). CY, cytoplasm; IB, PHA granule (inclusion body). The bar applies to all panels.

one of the major granule-associated proteins in *P. oleovorans* (20, 27).

Complementation of the *phaD* mutant GPo1001. To test if the GPo1001-dependent phenotype described above was attributable to disruption of the *phaD* gene or was due to another, unrecognized mutation or to a polar effect, we introduced the constructed broad-host-range *phaD* expression construct pHAD5 into the mutant GPo1001. PHA accumulation by GPo1001 containing pHAD5 was tested in minimal medium 0.1NE2 with 15 mM octanoate and kanamycin. The cells were induced in the early exponential phase (OD_{450} = 0.2) with 0.5 mM IPTG (isopropyl-β-D-thiogalactopyranoside). As shown in Table 2, pHAD5 was able to partly restore the PHA accumulation characteristics of the mutant GPo1001 and was able to restore the growth characteristics fully, leading to a cell dry mass accumulation which was slightly higher than that in the wild type.

We also did transmission electron microscopy studies with cells of the complemented mutant. As depicted in Fig. 2C, which shows a representative cell of GPo1001 harboring pHAD5, the cell size and the number and size of granules were similar to that found for wild-type cells (Fig. 2A).

Moreover, SDS-PAGE analysis of isolated granules of the mutant GPo1001 complemented with pHAD5 showed that PhaI was again attached to PHA granules (Fig. 3).

DISCUSSION

In this study it is shown for the first time that the *phaD* gene of *P. oleovorans* plays an important role in MCL PHA biosyn-

TABLE 3. Descriptive statistics for PHA granules of *P. oleovorans* GPo1000 and GPo1001 determined by analysis of electron micrographs[a]

Strain	No. of cells[b]	No. of PHA granules[c]	r_{gn}[d] (calculated) (μm)		Parameter determined	Parameter value			PHA (%, wt/wt) determined by:		
									EM[h]		GC measurements
			x	*y*		Range	Mean	Median	Mean	Median	
GPo1000	22	31	0.1–0.4	0.09–0.55	v_{gn} (μm^3)[e]	0.003–0.4	0.1	0.1			
	23	38			gn/cell[f]	1–5	2	1			
	23	32			(v_{gn} × gn/cell)/v_{cell}[g]	12–75	47	49	75.6	77.1	54.9
GPo1001	14	46	—[i]	0.02–0.19	v_{gn} (μm^3)	4×10^{-05}–0.03	0.003	0.0002			
	52	280			gn/cell	0–15	5	5			
	14	46			(v_{gn} × gn/cell)/v_{cell}	0–13	4	2	12.7	6.7	9.6

[a] Cultures of *P. oleovorans* GPo1000 and GPo1001 were grown on 0.1NE2 minimal medium containing 15 mM octanoate. Cells from stationary-phase cultures were prepared for electron microscopy as described in Materials and Methods. For each sample, 13 independent electron micrographs, each showing one or more bacterial cells, were chosen for analysis.
[b] Only sharply and completely depicted cells were chosen.
[c] Only sharply and completely depicted granules were chosen.
[d] Radius of PHA granules, calculated by multiplying the measured diameter factor (*x*, length; *y*, width) by the electron microscopy magnification.
[e] Average volume per PHA granule.
[f] Number of PHA granules per cell.
[g] Volume of PHA granules (average volume per PHA granule times number of granules per cell) per cell volume (percent).
[h] Calculated from micrographs, assuming a density of 1.05 g/ml and a conversion factor from cell volume to cell dry mass of 0.3.
[i] —, not determined, since PHA granules were spherical (assumption: a = b).

thesis in this organism. Upon insertion of the *tet* gene cassette in the *phaD* gene, we observed several effects on polymer accumulation in *P. oleovorans*. First, MCL PHA production in the *phaD* mutant was less than 20% of that in the wild type. The same effect was observed by Wieczorek et al. when the *phaP* gene in *Ralstonia eutropha*, encoding a phasin protein, was inactivated (29). In other species, such as *Rhodococcus ruber* and *P. putida*, reduction of PHA accumulation by disruption of genes coding for phasins has also been observed (19, 27).

To verify the *phaD* knockout in GPo1001, complementation of the mutant GPo1001 by introduction of a *phaD*-containing plasmid was done. Upon introduction of the *phaD*-containing construct, MCL PHA levels were partially restored (Table 1). Differences in the MCL PHA content between the complemented mutant and the wild type might be due to a changed level of expression of the extrachromosomal *phaD* gene or to a possible disruption of *phaC2* in GPo1001 caused by homologous recombination. Thus, we could demonstrate that the effects on MCL PHA accumulation in the mutant GPo1001 reported here were due to *phaD* inactivation rather than to a polar effect on downstream genes.

We initially concluded from the observations on reduced PHA production by *phaD* inactivation that *phaD* might code for a phasin protein. However, the data on PHA granule number, size, and shape in the *phaD* mutant were not in agreement with characteristics of other phasins studied by Wieczorek et al. (29) and Pieper-Fürst et al. (18). It has been shown for *R. eutropha* that upon inactivation of *phaP*, only one large PHA granule was built inside the cell (29), whereas *phaP* overexpression in the *phaP* mutant led to an increase in granule numbers compared to that for the wild type (29). As shown in Fig. 3 and Table 3, knockout of *phaD* increased the number of PHA granules, whereas complementation of the mutant by a *phaD*-harboring plasmid restored the number of granules to the wild-type level.

Moreover, in contrast to phasins described earlier (18–20, 27, 29), PhaD was not bound to PHA granules. As shown in Fig. 3, in the wild type we detected two major protein bands, representing the phasins PhaI and PhaF at 18 and 36 kDa, but no protein band of the expected size of the PhaD protein (23 kDa). This is in accord with previous studies which showed that PhaI and PhaF, but not PhaD, are major granule-associated proteins (20, 27). Moreover, the analysis of granule-associated proteins of the *phaD* mutant revealed that the protein pattern of PHA granules was changed and that the PhaI protein was missing (Fig. 3). The granule-associated protein pattern could be restored by introducing the *phaD* expression plasmid into the mutant GPo1001 (Fig. 3). Prevention of major granule-associated proteins, like PhaI, from binding to PHA granules has been shown to result in unspecific binding of cytoplasmic proteins to the granules and can therefore result in detrimental effects on metabolism or structural integrity of the cells (15, 26). This unspecific cytoplasmic protein binding to granules and removal from the cytoplasm might explain the change in the pattern of granule-associated proteins and might account for the smaller size of the *phaD* mutant cells (Fig. 2B). In

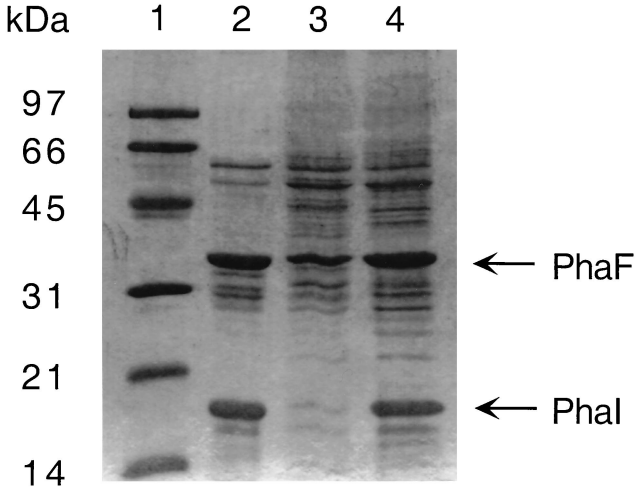

FIG. 3. PHA granule-associated proteins of *P. oleovorans* GPo1000 and GPo1001. Cells were cultivated in 0.1NE2 minimal medium containing 15 mM octanoate and were harvested in the early stationary phase. PHA granules were isolated and analyzed by SDS-PAGE. Granule-associated proteins of *P. oleovorans* GPo1000 (lane 2), GPo1001 (lane 3), and GPo1001(pHAD5) (lane 4) are shown. Lane 1, molecular mass standard proteins, with the masses indicated on the left. The PhaI and PhaF proteins are indicated.

agreement with this hypothesis, we found that complementation of GPo1001 with a *phaD*-harboring construct led to restoration of the cell size to the wild-type level (Fig. 2C).

In Table 2 we report that depolymerization of the PHA polymer in the mutant is significant, reducing the intracellular polymer content after 46 h of incubation to 1% (wt/wt), while depolymerization of PHA in wild-type cells is not detectable. It is known that during PHA synthesis the depolymerase is active to a certain extent (31). Doi reported that the rate of PHA accumulation in batch fermentation of *R. eutropha* was about 10 times higher than that of PHA degradation (6). Thus, an overall decrease of PHA in the mutant GPo1001 could be caused by a decreased rate of PHA biosynthesis while the rate of depolymerization remained constant.

In summary, we conclude that *phaD* is an important constituent of PHA biosynthesis but does not code for a granule-associated protein. Thus, we propose that it acts via an unknown mechanism, preventing expression or binding of major granule proteins, like PhaI, and leading to the observed effects on PHA accumulation.

ACKNOWLEDGMENTS

We thank Paul Walther and Ernst Wehrli for carrying out electron microscopy and Marcel Wolbers for professional expertise in statistical analysis. We thank Peter James for sequencing the N-terminal amino acids of the major granule-associated proteins and Wouter Duetz for helpful discussions.

This work was supported by grants from the Swiss Federal Office for Education and Science (BBW no. 96.0348).

REFERENCES

1. **Byrom, D.** 1987. Polymer synthesis by microorganisms: technology and economics. Trends Biotechnol. **5:**246–250.
2. **de Lorenzo, V., L. Eltis, B. Kessler, and K. N. Timmis.** 1993. Analysis of *Pseudomonas* gene products using *lacI*^{q}/P*trp-lac* plasmids and transposons that confer conditional phenotypes. Gene **123:**11–24.
3. **de Lorenzo, V., M. Herrero, U. Jakubzik, and K. N. Timmis.** 1990. Mini-Tn*5* transposon derivatives for insertion mutagenesis, promoter probing, and chromosomal insertion of cloned DNA in gram-negative eubacteria. J. Bacteriol. **172:**6568–6572.
4. **de Lorenzo, V., and K. N. Timmis.** 1992. Analysis and construction of stable phenotypes in Gram-negative bacteria with Tn5- and Tn10-derived minitransposons. Methods Enzymol. **31:**386–405.
5. **de Smet, M. J., G. Eggink, B. Witholt, J. Kingma, and H. Wynberg.** 1983. Characterization of intracellular inclusions formed by *Pseudomonas oleovorans* during growth on octane. J. Bacteriol. **154:**870–878.
6. **Doi, Y.** 1995. Microbial synthesis, physical properties, and biodegradability of polyhydroxyalkanoates. Macromol. Symp. **98:**585–599.
7. **Hohenberg, H., K. Mannweiler, and M. Müller.** 1994. High-pressure freezing of cell suspension in cellulose capillary tubes. J. Microsc. **175:**34–43.
8. **Huang, A. H. C.** 1992. Oil bodies and oleosins. Annu. Rev. Physiol. Plant Mol. Biol. **43:**177–200.
9. **Huisman, G. W., E. Wonink, R. Meima, B. Kazemier, P. Terpstra, and B. Witholt.** 1991. Metabolism of poly(3-hydroxyalkanoates) (PHAs) by *Pseudomonas oleovorans*. J. Biol. Chem. **266:**2191–2198.
10. **Klinke, S., Q. Ren, B. Witholt, and B. Kessler.** 1999. Production of medium-chain-length poly(3-hydroxyalkanoates) from gluconate by recombinant *Escherichia coli*. Appl. Environ. Microbiol. **65:**540–548.
11. **Kok, M.** 1988. Alkane utilization by *Pseudomonas oleovorans*. Ph.D. thesis. University of Groningen, Groningen, The Netherlands.
12. **Kraak, M. N., T. H. M. Smits, B. Kessler, and B. Witholt.** 1997. Polymerase C1 levels and poly(*R*-3-hydroxyalkanoate) synthesis in wild-type and recombinant *Pseudomonas* strains. J. Bacteriol. **179:**4985–4991.
13. **Laemmli, U. K.** 1972. Cleavage of structural proteins during the assembly of the head of bacteriophage T4. Nature **227:**680–685.
14. **Lageveen, R. G., G. W. Huisman, H. Preusting, P. Ketelaar, G. Eggink, and B. Witholt.** 1988. Formation of polyesters by *Pseudomonas oleovorans*: effect of substrates on formation and composition of poly-(*R*)-3-hydroxyalkanoates and poly-(*R*)-3-hydroxyalkenoates. Appl. Environ. Microbiol. **54:**2924–2932.
15. **Liebergesell, M., B. Schmidt, and A. Steinbüchel.** 1992. Isolation and identification of granule-associated proteins relevant for poly(3-hydroxyalkanoic acid) biosynthesis in *Chromatium vinosum* D. FEMS Microbiol. Lett. **99:**227–232.
16. **Miller, V. L., and J. J. Mekalanos.** 1988. A novel suicide vector and its use in construction of insertion mutations: osmoregulation of outer membrane proteins and virulence determinants on *Vibrio cholerae* requires *toxR*. J. Bacteriol. **170:**2575–2583.
17. **Murphy, D. J.** 1993. Structure, function and biogenesis of storage lipid bodies and oleosins in plants. Prog. Lipid Res. **32:**247–280.
18. **Pieper-Fürst, U., M. H. Madkour, F. Mayer, and A. Steinbüchel.** 1995. Identification of the region of a 14-kilodalton protein of *Rhodococcus ruber* that is responsible for the binding of this phasin to polyhydroxyalkanoic acid granules. J. Bacteriol. **177:**2513–2523.
19. **Pieper-Fürst, U., M. H. Madkour, F. Mayer, and A. Steinbüchel.** 1994. Purification and characterization of a 14-kilodalton protein that is bound to the surface of polyhydroxyalkanoic acid granules in *Rhodococcus ruber*. J. Bacteriol. **176:**4328–4337.
20. **Prieto, M. A., B. Bühler, K. Jung, B. Witholt, and B. Kessler.** 1999. PhaF, a polyhydroxyalkanoate-granule-associated protein of *Pseudomonas oleovorans* GPo1 involved in the regulatory expression system for *pha* genes. J. Bacteriol. **181:**858–868.
21. **Reynolds, E. W.** 1963. The use of lead citrate at high pH as electron opaque stain in electron microscopy. J. Cell Biol. **17:**208–212.
22. **Sambrook, J., E. F. Fritsch, and T. Maniatis.** 1989. Molecular cloning: a laboratory manual, 2nd ed. Cold Spring Harbor Laboratory Press, Cold Spring Harbor, N.Y.
23. **Schwartz, R. D., and C. M. McCoy.** 1973. *Pseudomonas oleovorans* hydroxylation-epoxidation system: additional strain improvements. Appl. Microbiol. **26:**217–218.
24. **Steinbüchel, A.** 1996. PHB and other polyhydroxyalkanoic acids, p. 405–464. *In* H.-J. Rehm and G. Reed (ed.), Biotechnology, vol. 6. VCH, Weinheim, Germany.
25. **Steinbüchel, A.** 1991. Polyhydroxyalkanoic acid, p. 123–213. *In* D. Byrom (ed.), Biomaterials. Novel materials from biological sources. Macmillan Publishers Ltd., Basingstoke, England.
26. **Steinbüchel, A., K. Aerts, W. Babel, C. Follner, M. Liebergesell, M. H. Madkour, F. Mayer, U. Pieper-Fürst, A. Pries, H. E. Valentin, and R. Wieczorek.** 1995. Considerations on the structure and biochemistry of bacterial polyhydroxyalkanoic acid inclusions. Can. J. Microbiol. **41**(Suppl. 1)**:**94–105.
27. **Valentin, H. E., E. S. Stuart, R. C. Fuller, R. W. Lenz, and D. Dennis.** 1998. Investigation of the function of proteins associated to polyhydroxyalkanoate inclusions in *Pseudomonas putida* BMO1. J. Biotechnol. **64:**145–157.
28. **Van Harreveld, A., and J. Crowell.** 1964. Electron microscopy after freezing on a metal surface and substitution fixation. Anat. Rec. **149:**381–386.
29. **Wieczorek, R., A. Pries, A. Steinbüchel, and F. Mayer.** 1995. Analysis of a 24-kilodalton protein associated with the polyhydroxyalkanoic acid granules in *Alcaligenes eutrophus*. J. Bacteriol. **177:**2425–2435.
30. **Witholt, B.** 1972. Method for isolating mutants overproducing nicotinamide adenine dinucleotide and its precursors. J. Bacteriol. **109:**350–364.
31. **Zinn, M.** 1998. Dual (C, N) nutrient limited growth of *Pseudomonas oleovorans*. Ph.D. thesis. ETH Zürich, Zürich, Switzerland.